

# Application and verification of ECMWF products 2019

*Hellenic National Meteorological Service (HNMS)  
Dimitra Boucouvala, I.Kouroutzoglou and Ch. Kolyvas*

## **1. Summary of major highlights**

The ECMWF products are widely used in HNMS and are essential tools for our daily forecast.

The medium-range weather forecasts at the HNMS are based primarily on the deterministic ECMWF forecast. Both the 00 UTC and 12 UTC cycles of the ECMWF forecasts are received daily in the current resolution. For short-range forecasting and for observation of local characteristics of weather patterns in Greece, the output of the limited area models is used in conjunction with the ECMWF products.

Daily verification is performed for the surface and upper-air fields of the IFS products as well as for the high-resolution limited area model (COSMO-GR at 4 and at 1km) that are used by the HNMS forecasters. In addition, the relative performance of the models is subject to intercomparison.

## **2. Use and application of products**

### **2.1 Direct use of ECMWF Products**

The HNMS forecasting centre uses ECMWF products in conjunction with the products of its limited area models for the general 7-day forecast that is provided to the public as well as for the sea state forecast for the Eastern Mediterranean and, finally, the forecast for aeronautical purposes. The IFS forecast products are also consulted by the forecaster on duty and used to complete the awareness report for the European MeteoAlarm website.

The EPS products (plumes, meteograms, ensemble probability maps) are retrieved daily from the ECMWF website and are of particular value to the HNMS forecasters, especially the d+4 to d+7 forecast where the value of the deterministic forecasts is substantially reduced). An increasingly popular ECMWF product at the HNMS is the Extreme Forecast Index (EFI) for temperature and precipitation. As a measure of the distance from the climatological value (mean), the EFI maps are directly related to severe weather events. The monthly (and weekly) anomalies and seasonal forecasts are not used operationally but only for consultative or research purposes.

### **2.2 Other uses of ECMWF output**

#### *2.2.1 Post Processing*

The HNMS implements a method improving the temperature minimum and maximum forecast values for 50 locations in Greece (position of the stations) on a daily basis. This method uses a Kalman filtering technique, which is based on non-linear polynomials, incorporating all available quality-controlled observations in combination with the corresponding NWP data of the IFS model as well as from the limited area model COSMO-GR (4 and 1km). Application of the filter helps improve the temperature forecasts by eliminating possible systematic errors. The same technique is also used with the dew point temperature data (minimum and maximum) in order to correct biases related to relative humidity.

#### *2.2.2 Derived fields*

A wide range of derived fields are produced from the ECMWF model outputs (e.g. meteograms) for visualisation, issue of aeronautical forecasts and other applications at the forecasting center.

#### *2.1.3 Modeling*

ECMWF model output provides the lateral and boundary conditions for the execution of the daily simulations of the HNMS limited area model (COSMO-GR, WAM). As an option, ECMWF model output can also be used to provide the necessary input for the MOTHY trajectory model.

MOTHY is a sea pollution model (e.g. Daniel, 1996), which is applied in cases of oil spills in the eastern Mediterranean Sea, that HNMS is responsible for. It is based on the numerical weather predictions of the ECMWF model, either the 00:00 UTC cycle or the 12:00UTC cycle. The data used as input are the surface wind speed and the sea surface pressure, (and the two meters temperature as an option). The model provides the possible trajectories (locations) of oil (or floating objects) transport as well as the percentage of the oil spill that will reach the coast or the seabed. The HNMS operates MOTHY as part of the Marine Pollution Emergency Response Support System (MPERSS) for the Marine Pollution Incident (MPI) Area III East, which includes the eastern Mediterranean Sea.

Finally, the ECMWF deterministic model provides the necessary initial conditions to drive a wave forecast model (WAM) as an alternative option to COSMOGR. The wave forecast of the HNMS is based on the ECMWF version of the WAM (CYCLE 4) model. It is a third generation wave model which computes spectra of random short-crested wind-generated waves and is one of the most popular and well tested wave models. Verification of the calculated wave height and direction has been implemented with the use of observations taking by the buoys positioned around the Greek Seas (POSEIDON system).

### **3. Verification of ECMWF products**

In order to determine the quality of the NWP products at the Hellenic National Meteorological Service (HNMS), a verification process is applied based on a tool that was developed through the **CO**nsortium for **S**mall-scale **MO**deling (COSMO). This operational conditional verification tool, known as **VER**ification **S**ystem **U**nified **S**urvey (VERSUS), the development of which was coordinated by the Italian Meteorological Service, is currently used by the HNMS for all verification activities concerning the weather forecast models. The operational verification system at the HNMS has been expanded to include verification of ensemble forecasts as well as wave model forecasts.

In the same time for spatial verification purposes, in a test case base, VAST (VERSUS Additional Statistical Techniques) software package, which was also developed by the COSMO consortium is employed as it offers a number of neighborhood verification tools (Gofa et al. 2018).

Monthly and seasonal verification is performed for the surface and upper-air fields of the IFS products as well as for the high-resolution limited area model (COSMO-GR at 4 and at 1km) that are used by the HNMS forecasters. In addition, the relative performance of the models is subject to intercomparison. The operational verification system at the HNMS has been expanded to include verification of ensemble forecasts derived by -range ensemble prediction systems as well as wave model forecasts.

#### **3.1 Objective verification**

##### *3.1.1 Direct ECMWF model output*

The forecasted values of weather parameters are compared with synoptic meteorological data from the HNMS operational network of stations and a range of statistical scores is calculated on a daily, monthly and yearly basis. The surface verification is performed by using the SYNOP data from the most reliable surface stations, every 3 or 6 hours.

The continuous variables that are routinely verified are the 2m temperature, 2m dew point temperature, Mean Sea Level pressure, wind speed and cloud cover. For dichotomic parameters such as precipitation, the 6-, 12- and 24h-hour precipitation amounts are verified using indices from the respective contingency tables for the 72-hour forecast horizon. The thresholds for the precipitation amounts range from 0.2mm up to 30mm, accumulated in different time ranges. Only a small selection of statistics for 12h is presented in the current report and correspond to the four seasons.

The RMSE and Bias scores are calculated for every forecast cycle, every 3 hours from the t+3 to the t+120 forecast hour (here presented up to 72h) for every synoptic station, indicating the degree to which the forecast values differ from the observations. The scores, which are averaged over all stations, are presented below. The verification was performed for every season (JJA2018-MAM2019), ECMWF/IFS statistics are represented with the red lines. Our local model COSMOGR (4 and 1km resolution) is also depicted in the graphs. The main findings are as follows:

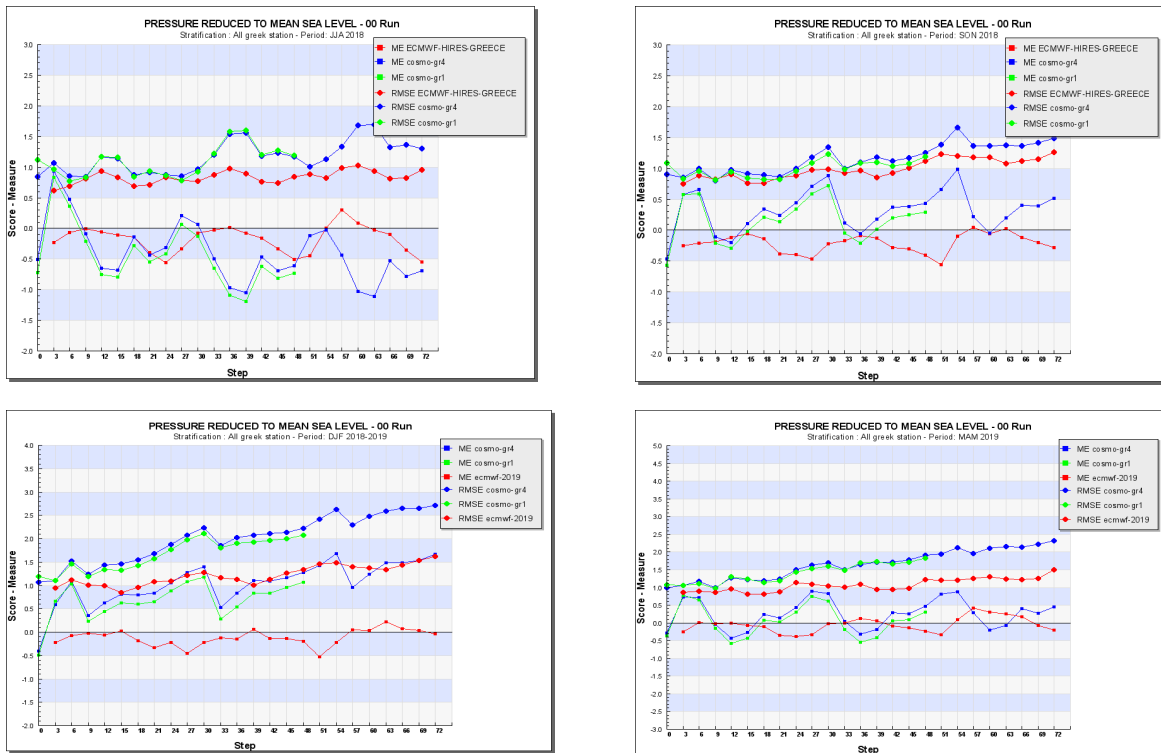
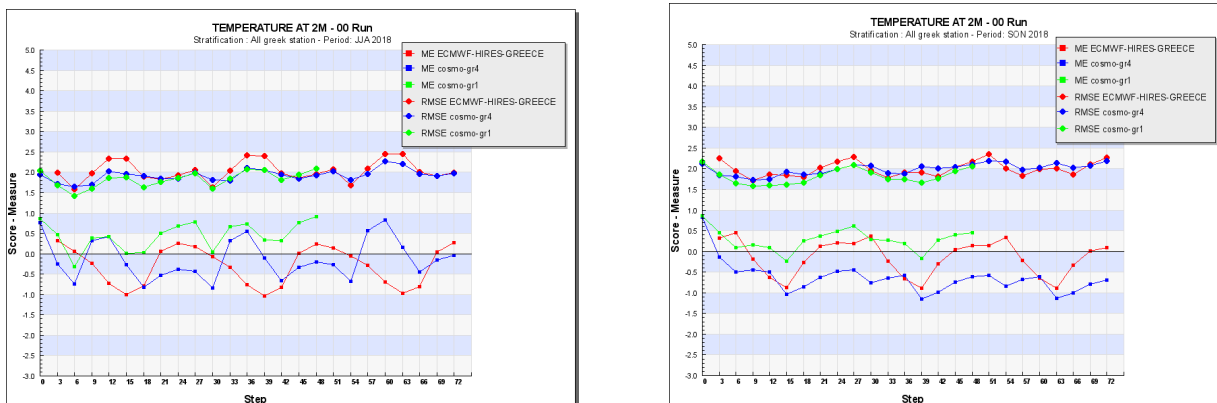


Fig.1 RMSE and Bias (ME) score for MSLP from all models (00UTC run) calculated and presented for every season for JJA18 (left top), SON18 (right top), DJF19 (left bottom) and MAM19 (right bottom)

**Mean Sea Level Pressure:** (Fig. 1) A slight propagation of the error (RMSE) with forecast time is evident for all seasons especially in DJF. The IFS bias values indicate a slight MSLP underestimation at nighttime in all seasons, but the score is better in the daytime. Lower bias values in DJF and MAM.



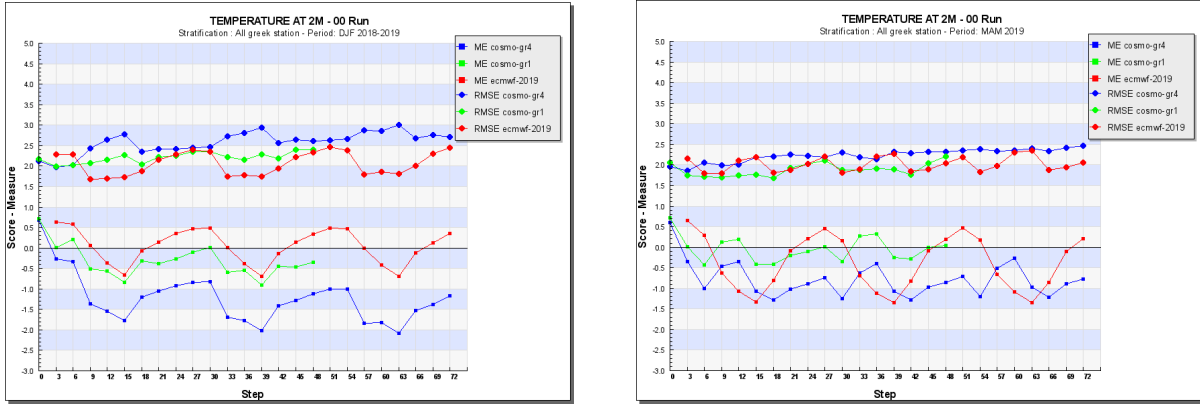


Fig.2 RMSE and Bias scores for 2m Temperature from all models (00UTC run) calculated and presented for every season

**2m Temperature:** A clear diurnal cycle of the Bias values is a characteristic of all seasons. (Fig. 2). IFS underpredicts the daytime temperature values to up to 1 K (in the summer) and slightly overpredicts nighttime values especially in winter. RMSE also exhibits a slight diurnal variation with time with slightly higher values at night in DJF and daytime in JJA. The average RMSE for all periods is approximately 2K.

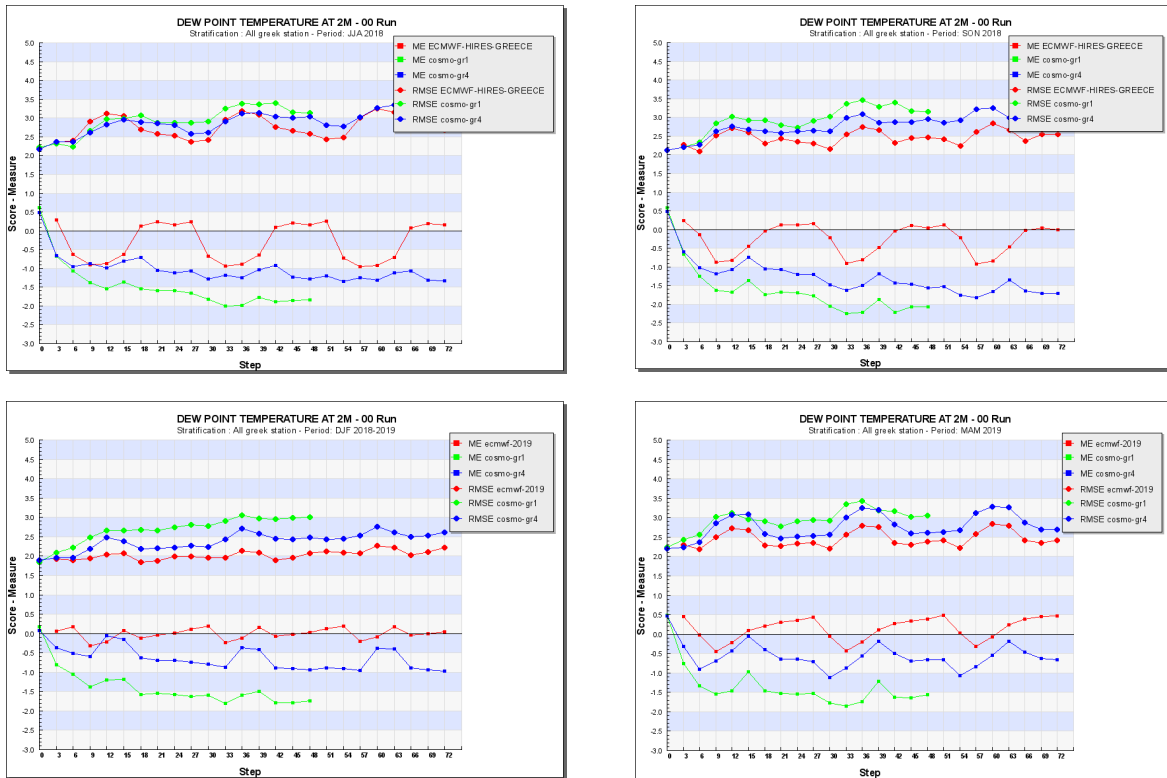


Fig.3 RMSE and Bias scores for 2m Dew Point Temp (seasonal) from the all models (00UTC run)

**2m Dew Point Temperature:** The diurnal cycle is evident in the Bias values in all seasons except for DJF. The DPT is mainly underestimated the warm hours of the day especially in the summer and fall. The bias is almost zero in the winter. RMSE values are lower in the winter season (Fig. 3).

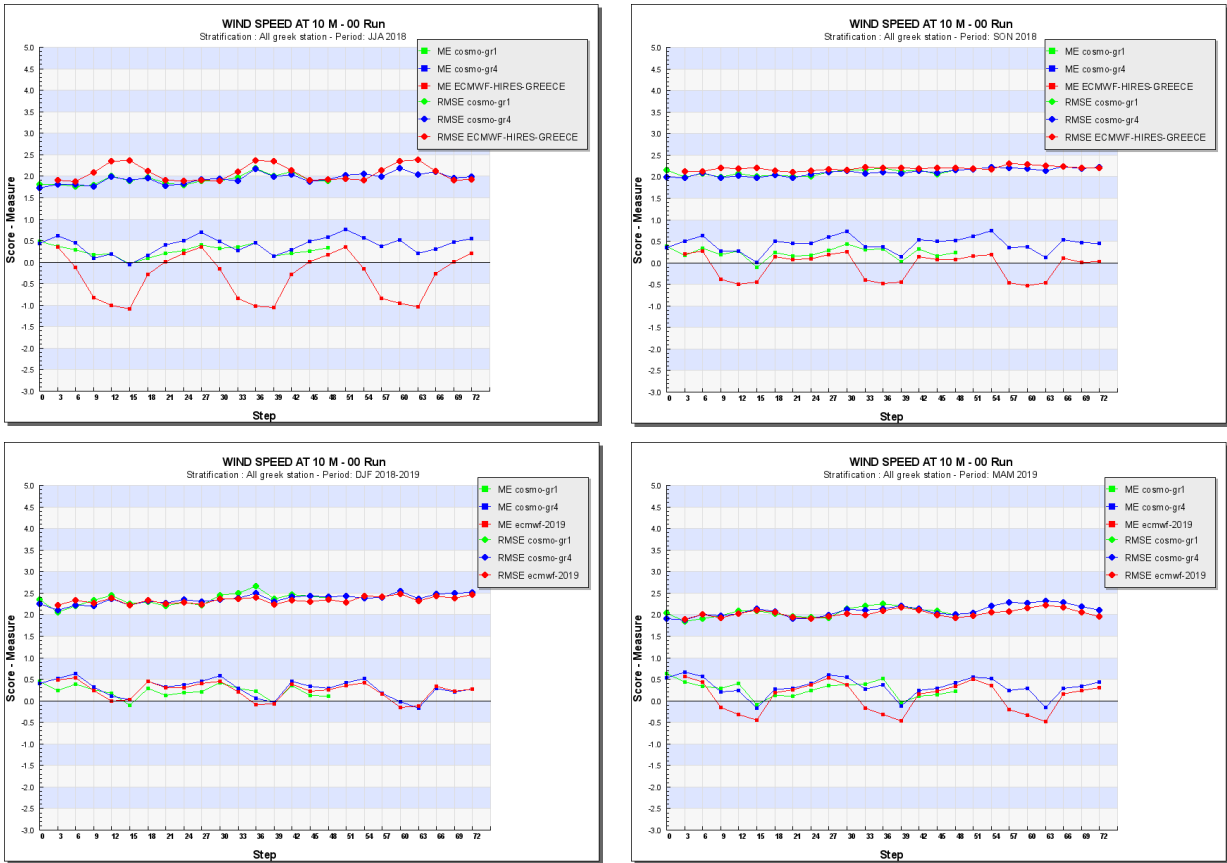
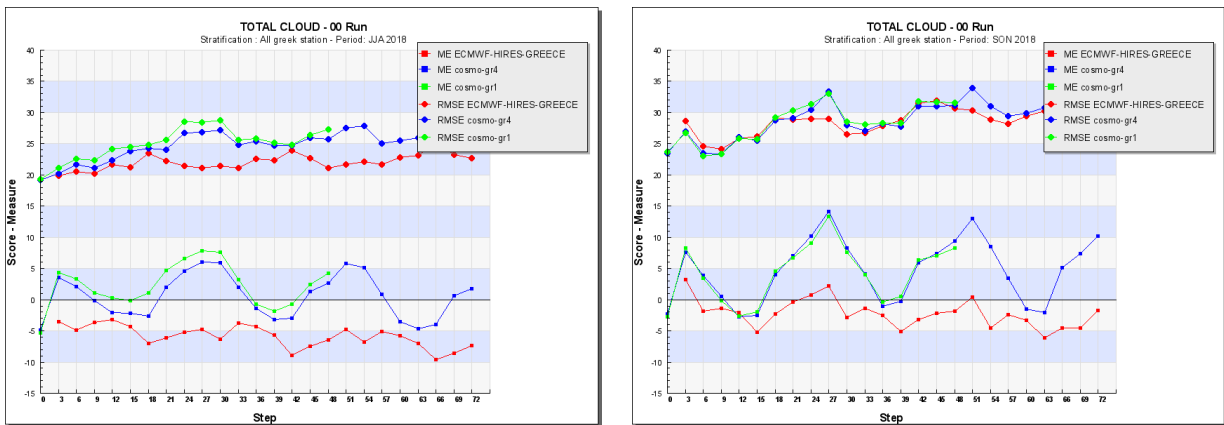


Fig.4 RMSE and Bias scores for 2m for 10m Wind speed from the all models (00UTC run)

**10m Wind Speed:** RMSE behaviour and values are almost constant for all seasons with values around 2 m/s with a clear daily cycle in the Bias values for JJA which show some underestimation of winds in warm hours (Fig. 4).



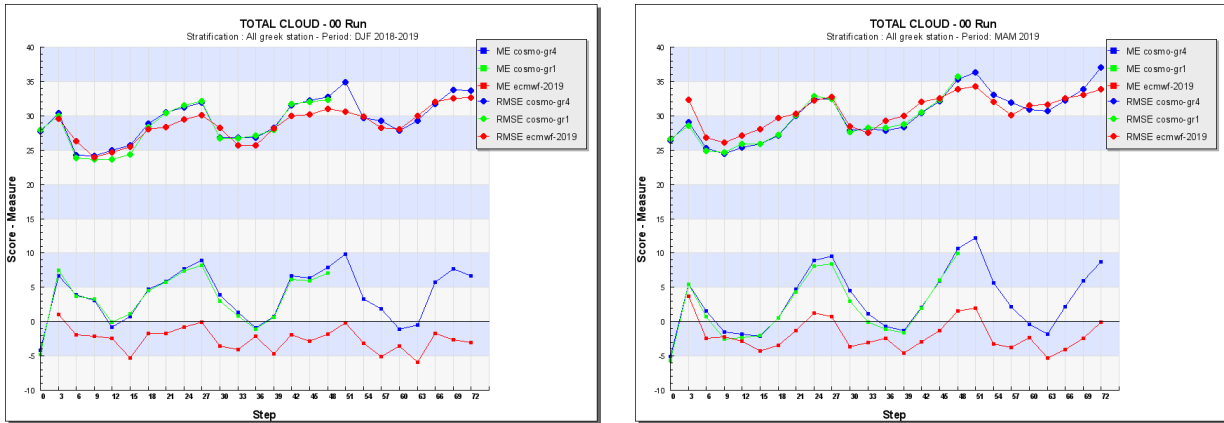


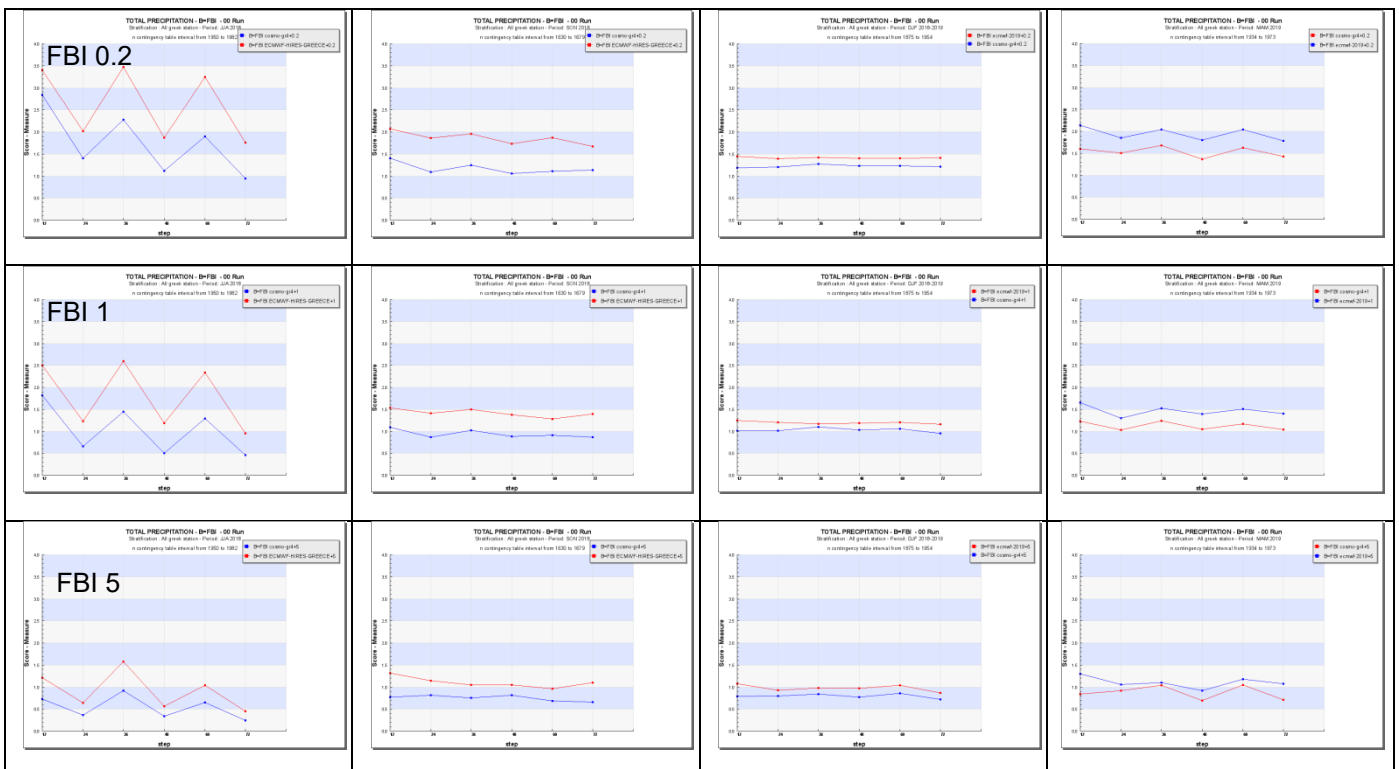
Fig.5 RMSE and Bias scores for Cloud Cover from all models (00UTC run)

**Cloud Cover:** A general slight underestimation of cloud cover percentage from IFS model is apparent in all seasons as well as a relatively weak daily cycle of the bias. The RMSE values slightly increase with lead time with better performance during the summer season when weather conditions are more stable and cloud cover amount is in general decreased (Fig.5).

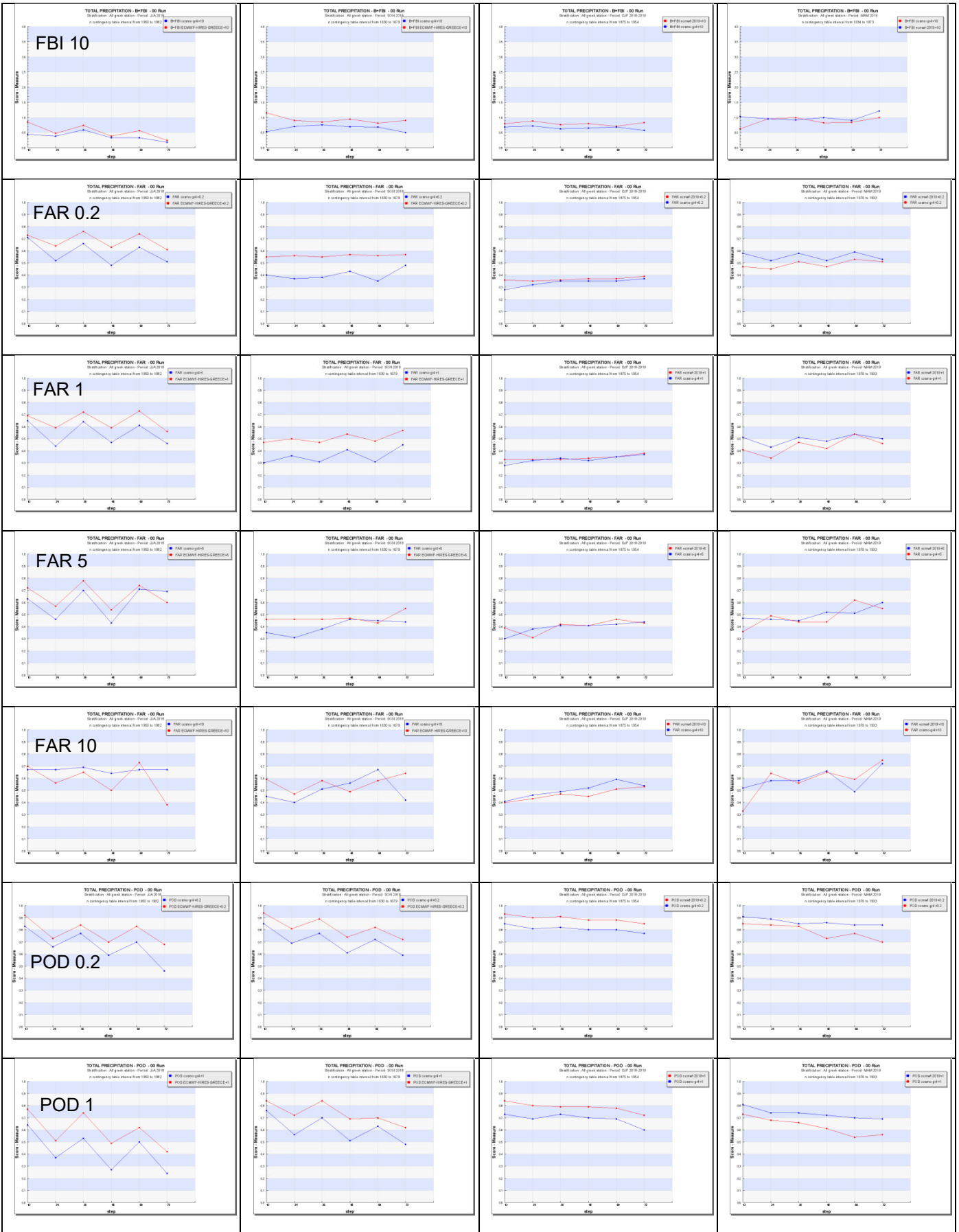
**Precipitation:**

Precipitation is commonly accepted as the most difficult weather parameter to correctly predict in terms of its spatial and temporal structure due to its stochastic behaviour and any connection with specific weather systems is greatly appreciated by forecasters. The 12h-hour precipitation amounts were verified for this study and the thresholds for the precipitation amounts ranged from 0.2mm up to 10mm accumulated over 12h time interval. For each threshold a number of scores were calculated to provide insight into model behaviour. The scores chosen for this report are the FBI (Bias), the FAR (False Alarm Ratio) and POD (Probability of Detection). Scores are presented for thresholds of 0.2,1,5,10mm (rows) for all seasons (columns).

JJA SON DJF MAM



# GREECE



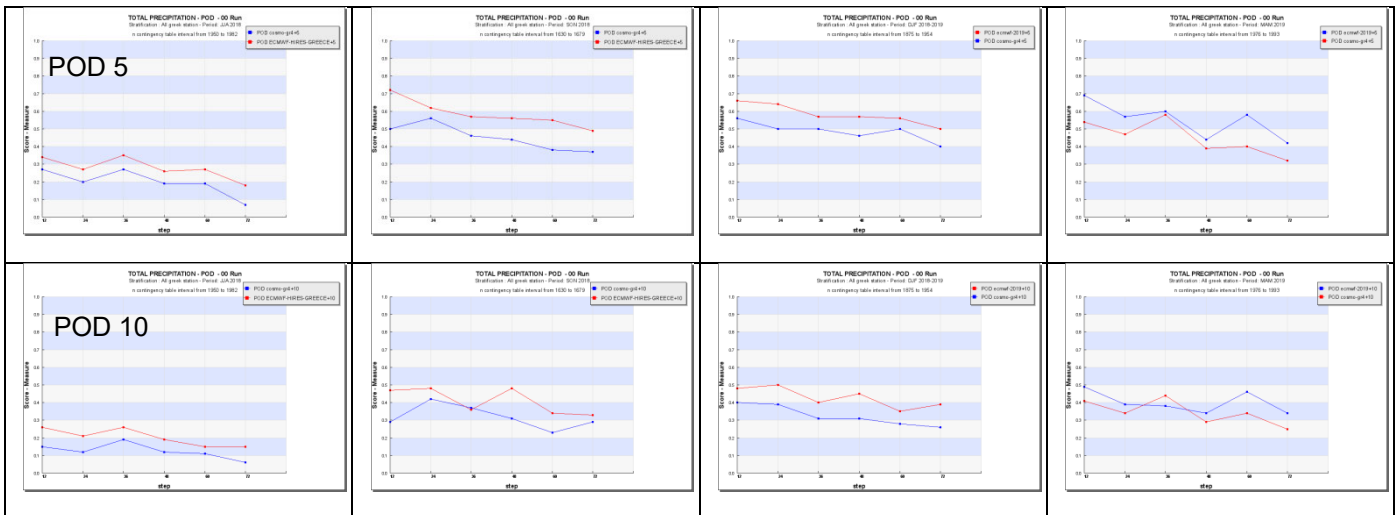


Fig.6 Scores for 12h precipitation with forecast time (x axis): FBI, (rows 1-4) FAR (rows 5-8) and POD (rows 9-12) for threshold 0.2, 1, 5, 10mm on each row on each score respectively for JJA, SON, DJF, MAM (columns from left to right). Red line represents IFS-ECMWF

**FBI:** Overestimation of precipitation events (larger for 00-12h) for low thresholds, with a clear diurnal cycle in warm seasons especially JJA. For higher thresholds, there is a slight underestimation of events and a weaker diurnal cycle.

**FAR:** Diurnal cycle in warm seasons especially in JJA with higher values for 00-12h especially for low thresholds. No significant difference of FAR values with increasing threshold and forecast time. Less false alarms are in DJF where no diurnal cycle is apparent.

**POD:** Diurnal cycle in warm seasons especially in JJA with higher values for 00-12h and low thresholds. POD values are higher in DJF with no diurnal cycle. POD values drop with increasing threshold and forecast time.

## 3.2 Subjective verification (by I. Kouroutzoglou)

### 3.2.1 Subjective scores

The most important features of unsuccessful precipitation forecasting are the following:

a) Underestimating of precipitation totals over Eastern –windward parts of Greece:

- i. when the 500 hPa prevailing flow is SW, or
- ii. a cold front crosses the country from the west and mainly SW, considering that the orography of continental Greece distorts the thermodynamic structure of the low level frontal activity
- iii. Extensive low level baroclinic zones without necessarily be combined to organized frontal activities, mainly from Northern Africa,

b) On the contrary, overestimating of precipitation totals snowfall, in particular over NE mainland Greece,

c) Often unsuccessful tracking of the movement of extensive, quasi-stationary cut-off lows (500hPa), situated over a wide area in the Central - Eastern Mediterranean - secondary upper level cyclogenesis. For example when a warm upper level anticyclone forms in the Atlantic or the Western European area and upper level downstream development rejuvenates the pre-existed quasi-stationary cut-off low under the effect of a mobile polar front jet streak and the strengthening of the respective transverse ageostrophic circulations,



d) Unsuccessful simulation of diabatic heating in the form of surface sensible and latent heat fluxes from the sea during the transitional time periods between warm and cold sea (Lolis et al., 2004)

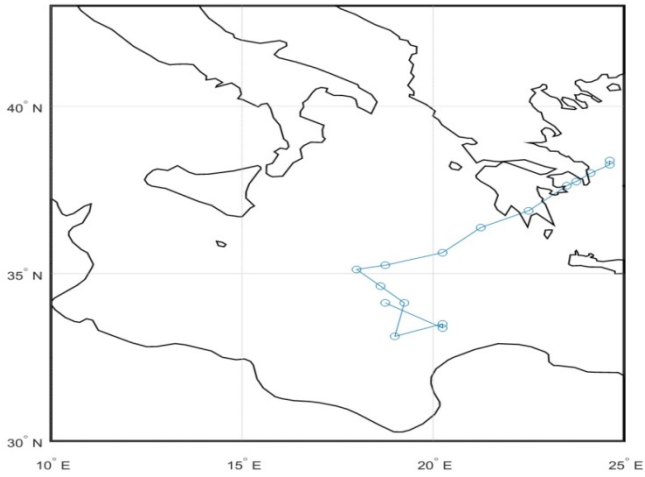
e) Unsuccessful simulation of the transformations of surface frontal activities in cases where the absence of organized conveyor belts and wind component perpendicular to the frontal activities does not allow the surface depression to follow the typical life cycle of a mid-latitude surface depression from the incipient to the mature stage. In these cases the dissipation of the cyclone's warm front and the formation of comma clouds or occluded fronts with persistence over a specific area, being steered by a stationary or quasi-stationary upper level cyclone, lead to problematic forecasts of the surface front's movement,

f) The general synoptic behavior of June and July 2018 over the Mediterranean area, allows us to expand the comment of paragraph (d) for the period of cold sea, as well. The increased frequency of establishment of upper level blocking anticyclones in the Atlantic or of Western Europe and the resultant shift of the atmospheric circulation from zonal to meridional, allowed the southward propagation of upper level deep cyclonic circulations (often detected even in the 850hPa isobaric level) towards the southern parts of Mediterranean area, including the Eastern Mediterranean and Greece.(Prezerakos et al, 1999) Despite the fact that climatologically the air-sea interaction does not favor instability over the Eastern Mediterranean Sea surface during summer, lightning activity and thunderstorms were observed over the Ionian and the Aegean Sea during the above mentioned episodes between June and July 2018, implying that upper level dynamic forcing managed to overcome the tendency of a stable low level stratification over the sea surface. In the majority of these cases the ECMWF forecast precipitation failed to simulate effectively the cloudiness and the precipitation amounts over the sea and especially over the southern parts of the Aegean and Ionian Seas. Nevertheless, it is also a question whether the sign of the heat fluxes from the sea is reversed (from negative – instability to positive – stability), except the influence of the above mentioned upper level forcing. Although the air-sea interaction does not favor climatologically the instability over the Eastern Mediterranean Sea during summer, this does not mean that in any synoptic type  $T_{air} - T_{sea} > 0$ . For example, in cases of surface and low level NW flow over Greece (existence of surface cyclogenesis and probably frontogenesis over the Eastern Europe and the Black Sea), the temperature of the surface air mass advected from the Eastern Balkans towards the Aegean Sea will probably be smaller than the SST over the Aegean Sea (especially during the night hours). In these cases both the upper level dynamic processes and the respective surface and low level diabatic ones, will positively operate in order to have  $\omega < 0$  over the sea surface and the combination of potential and convective instability. Koutoutzoglou et al.(2018)

### .3.2.2 Case studies

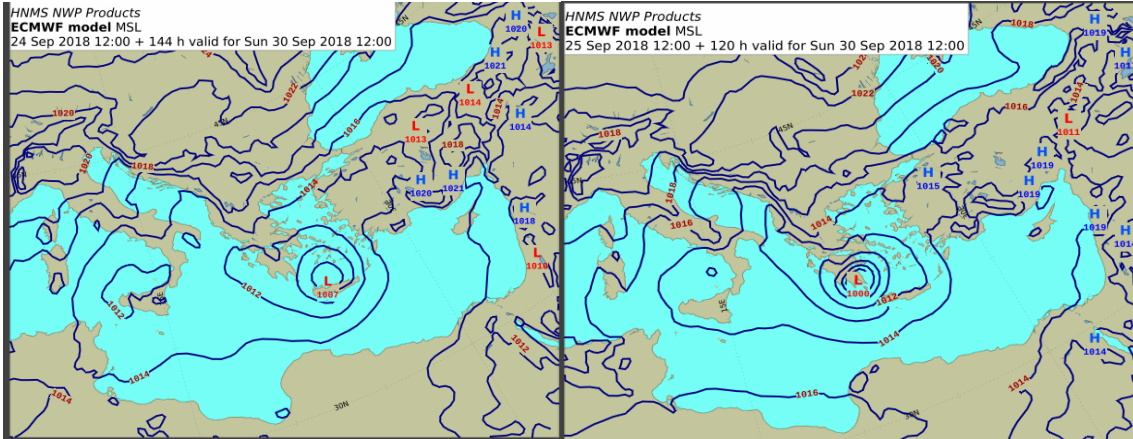
A case of particular interest including the main aspects of the above mentioned comments is the Mediterranean tropical-like cyclone of 28-30 September 2018 in Central Mediterranean affecting Greece which strong weather phenomena. The first stage of the episode was the formation of a frontal depression with characteristics of an explosive cyclone over the coasts of Libya during the time period between 27 to 28 of September 2018 and the second stage was the transition into a Mediterranean cyclone during the period between 28 to 29 of September 2018, according to the analysis made by the thermodynamic analysis made by the HNMS including the calculation of the parameters determining the thermal symmetry and the warm core structure in both the upper the lower troposphere. The track based on the ECMWF analyses is presented in the next Figure.

## CYCLONE TRACK BASED ON THE ECMWF ANALYSES

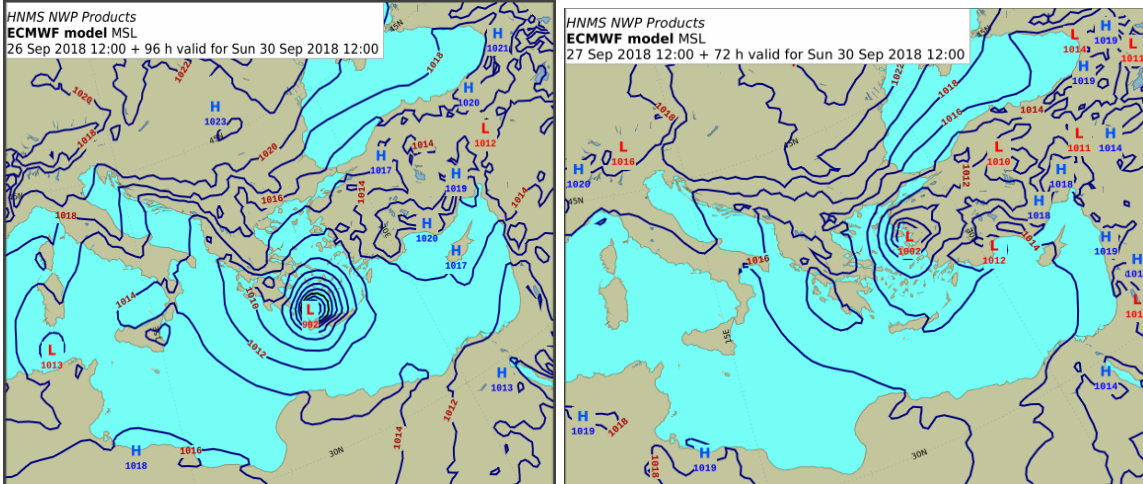


Despite the fact that this synoptic situation was affected by the formation and the evolution of a sub-synoptic vortex with individual thermodynamic characteristics and structure increasing the forecast uncertainty, one should probably waiting a more sufficient simulation of the kinematic characteristics and the deepening rates of the cyclone, for example 3 or 4 days before the initiation of the phenomenon. Nevertheless, the operational HRES ECMWF model presented significant differences between the successive runs from the 24<sup>th</sup> of September, as shown in the next figures.

**MSLP for 30/09 12UTC / 24/09 12UTC MODEL RUN      MSLP for 30/09 12UTC / 25/09 12UTC MODEL RUN**

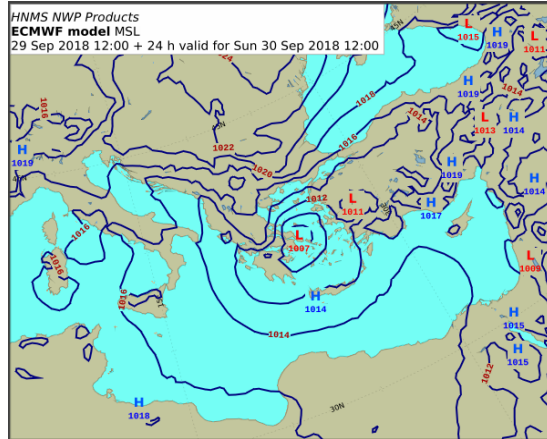
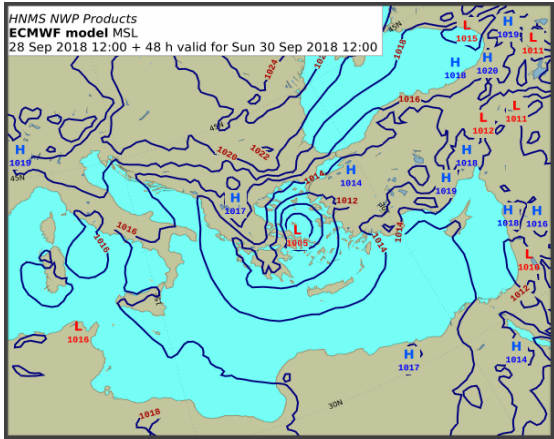


**MSLP for 30/09 12UTC / 26/09 12UTC MODEL RUN      MSLP for 30/09 12UTC / 27/09 12UTC MODEL RUN**



**MSLP for 30/09 12UTC / 28/09 12UTC MODEL RUN**

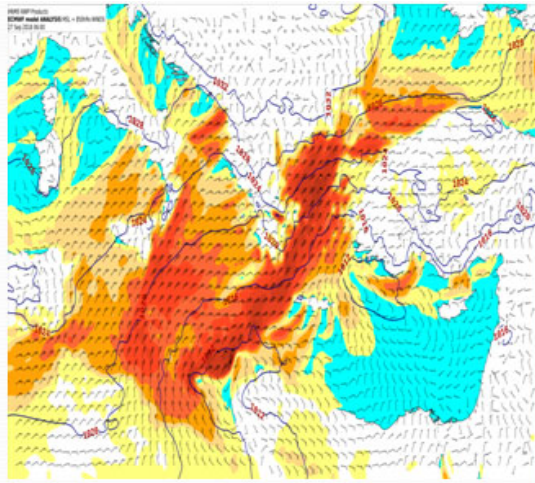
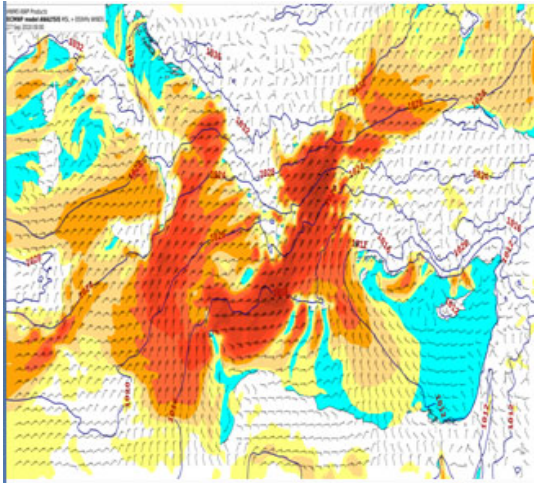
**MSLP for 30/09 12UTC / 29/09 12UTC MODEL RUN**



In the next figures the MSLP analyses along with the 850hPa winds are presented in order to assist the evaluation of the previous forecast charts.

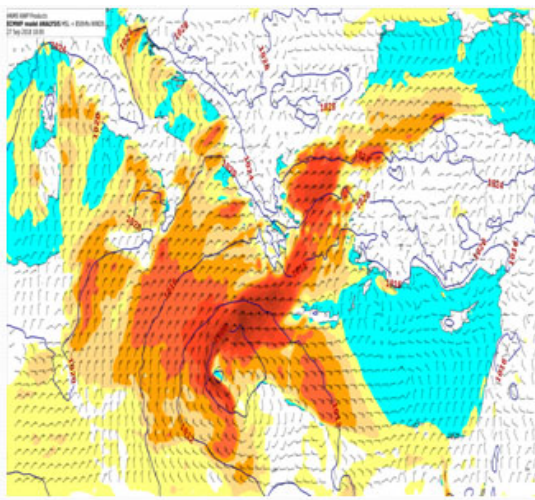
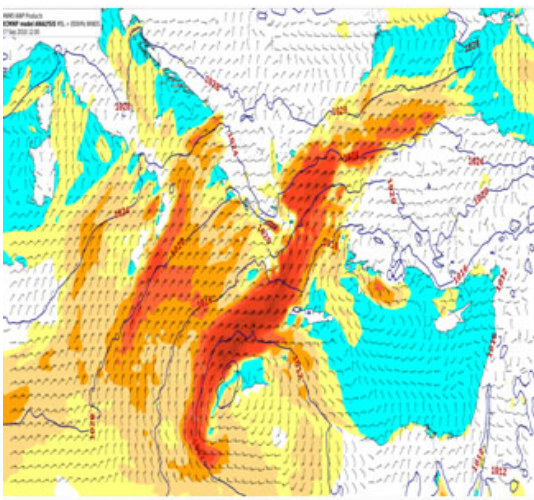
**MSLP/850HPa winds for 27/09 00UTC**

**MSLP/850HPa winds for 27/09 06UTC**

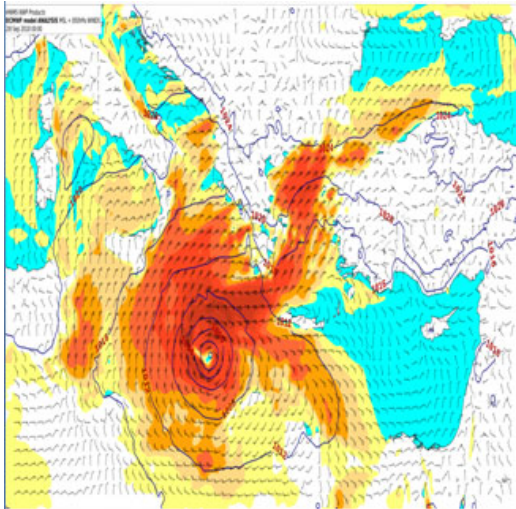


**MSLP/850HPa winds for 27/09 12UTC**

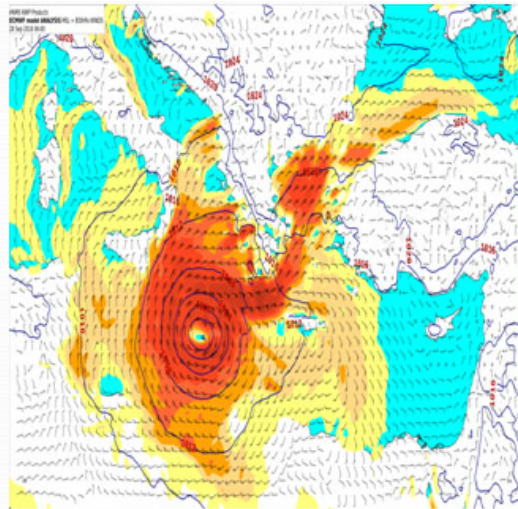
**MSLP/850HPa winds for 27/09 18UTC**



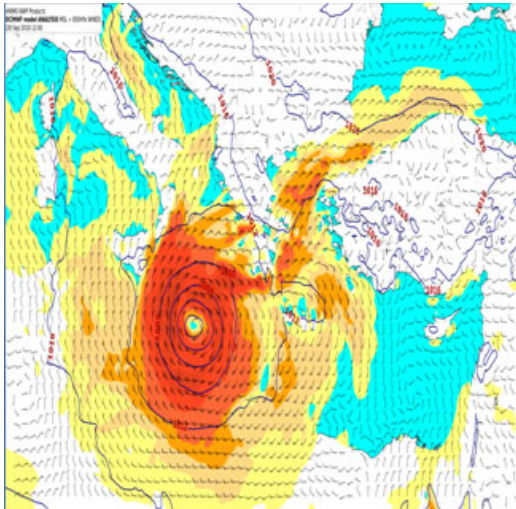
**MSLP/850HPa winds for 28/09 00UTC**



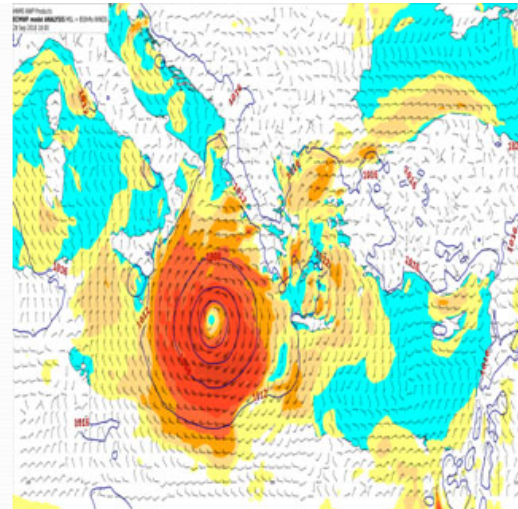
**MSLP/850HPa winds for 28/09 06UTC**



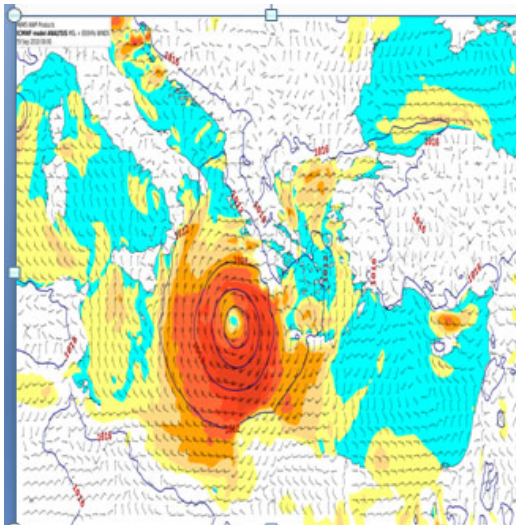
**MSLP/850HPa winds for 28/09 12UTC**



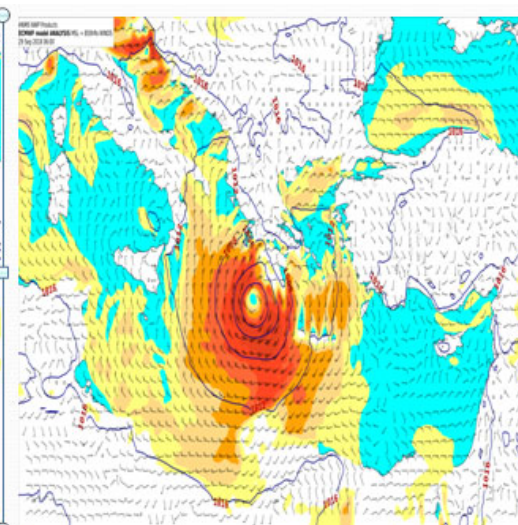
**MSLP/850HPa winds for 28/09 18UTC**



**MSLP/850HPa winds for 29/09 00UTC**

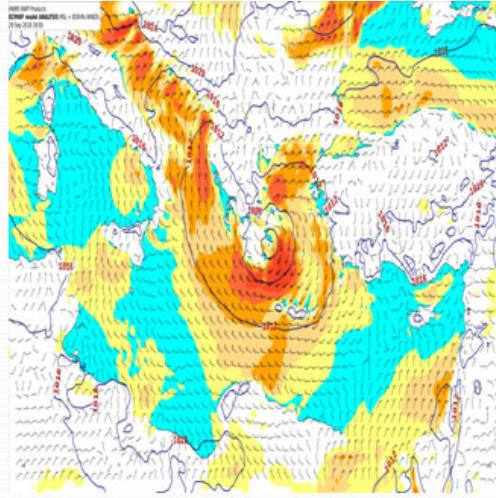
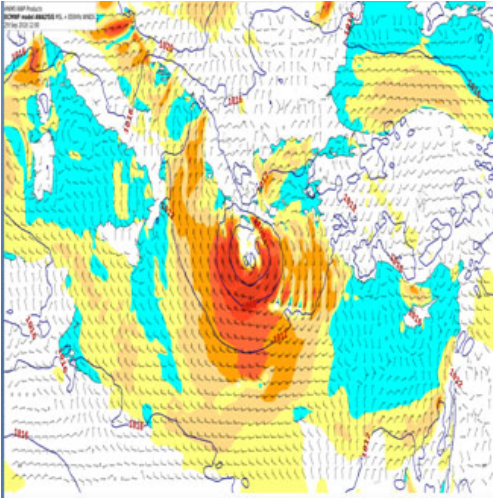


**MSLP/850HPa winds for 29/09 06UTC**



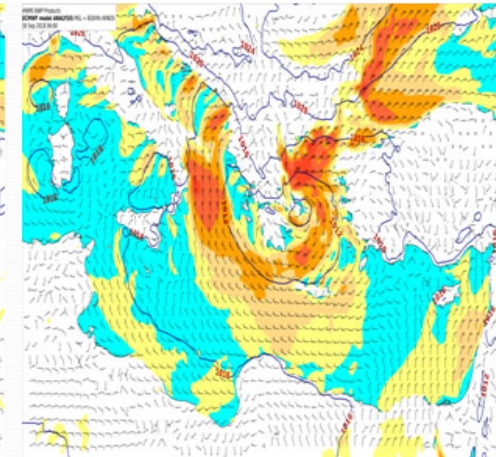
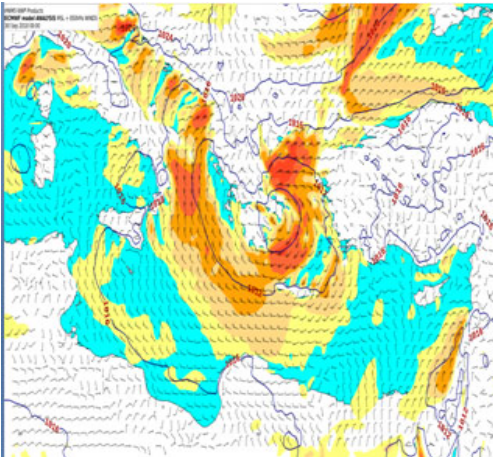
**MSLP/850HPa winds for 29/09 12UTC**

**MSLP/850HPa winds for 29/09 18UTC**



**MSLP/850HPa winds for 30/09 00UTC**

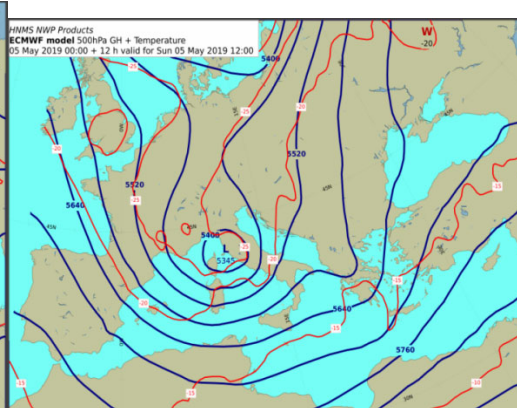
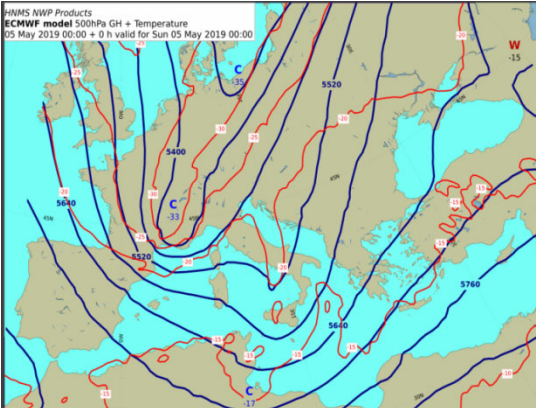
**MSLP/850HPa winds for 30/09 06UTC**



A second synoptic case with unsatisfactory simulation of precipitation over Greece was the case during the time period between 04-06 May 2019. The non-effective simulation occurred in both an area of a low level baroclinic zone (with characteristics of a frontal wave) over the Southern Aegean Sea and the Crete and the Ionian Sea where an extended upper level cyclonic circulation in Central Mediterranean was propagating slowly towards the western parts of Greece with surface frontal activity over the Ionian Sea.

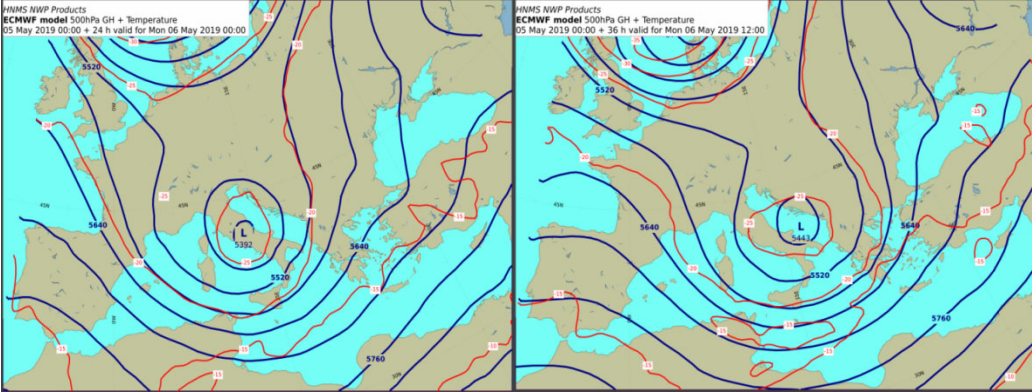
**500hPa GH-T forecast for 05-05-2019 00UTC**

**500hPa GH-T forecast for 05-05-2019 12UTC**

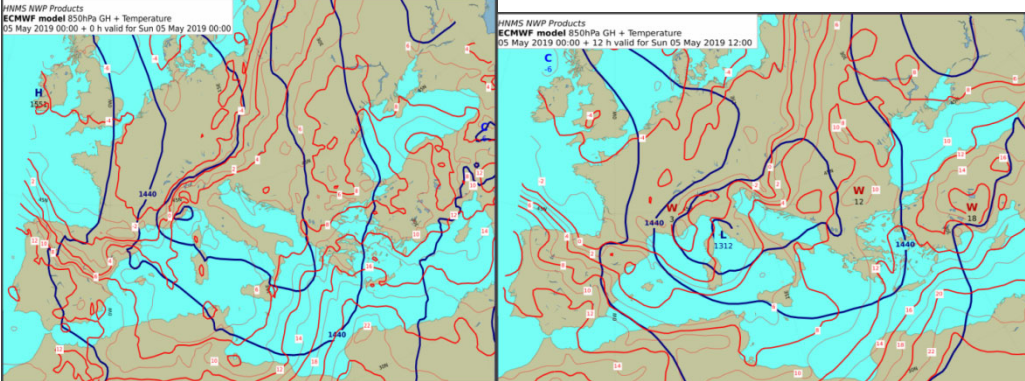


GREECE

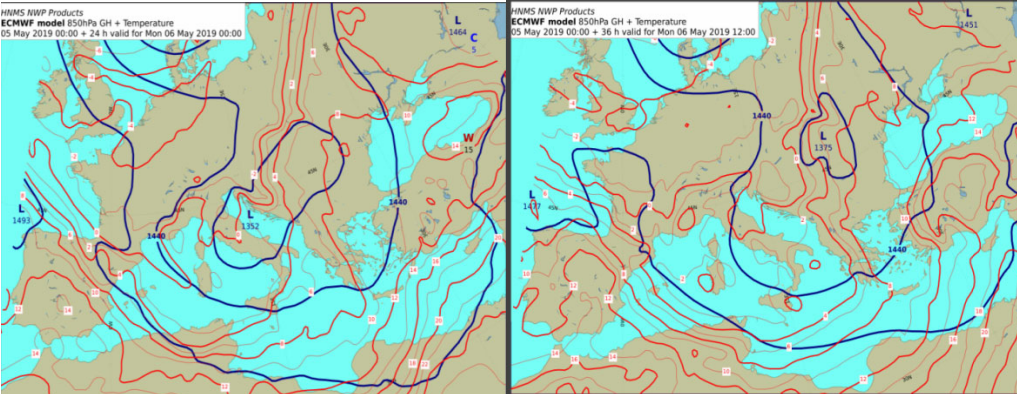
**500hPa GH-T forecast for 06-05-2019 00UTC    500hPa GH-T forecast for 06-05-2019 12UTC**



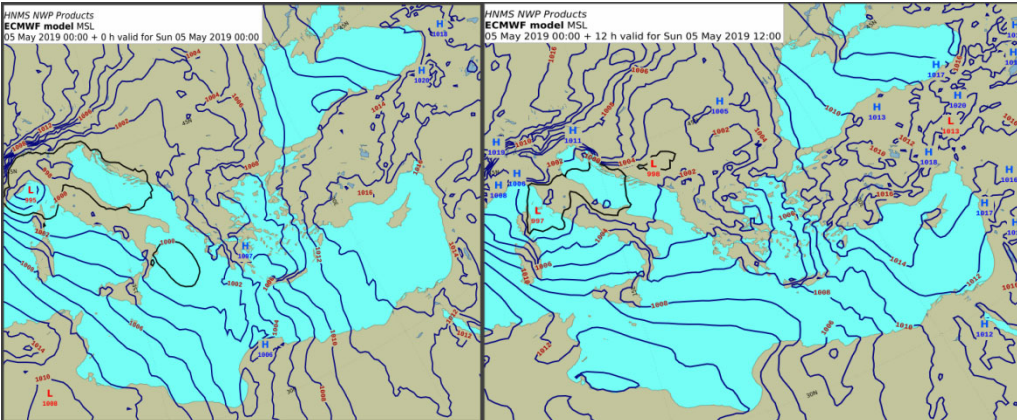
**850hPa GH-T forecast for 05-05-2019 00UTC    850hPa GH-T forecast for 05-05-2019 12UTC**



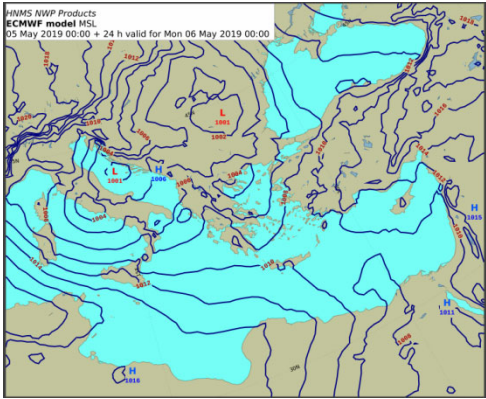
**850hPa GH-T forecast for 06-05-2019 00UTC    850hPa GH-T forecast for 06-05-2019 12UTC**



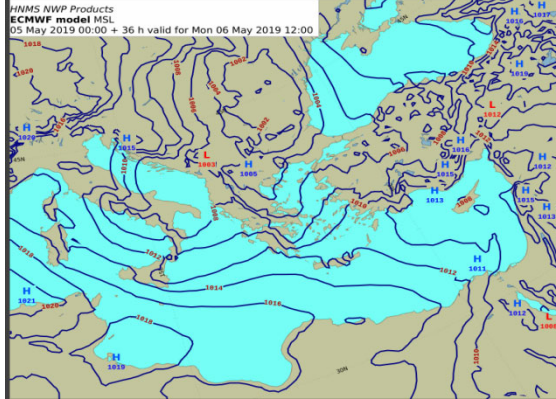
**MSLP forecast for 05-05-2019 00UTC    MSLP forecast for 05-05-2019 12UTC**



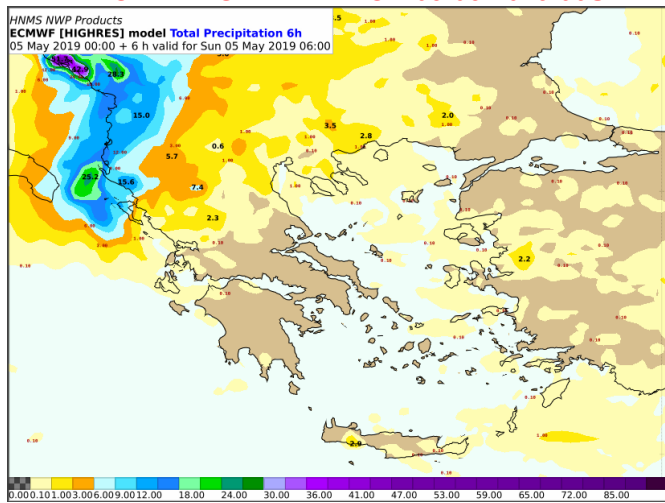
**MSLP forecast for 06-05-2019 00UTC**



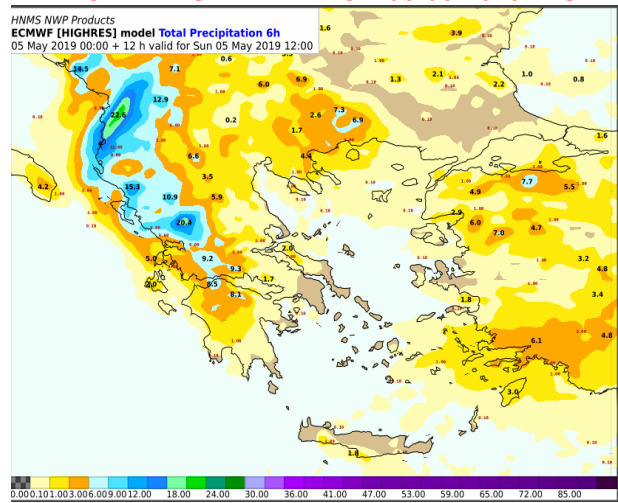
**MSLP forecast for 06-05-2019 12UTC**



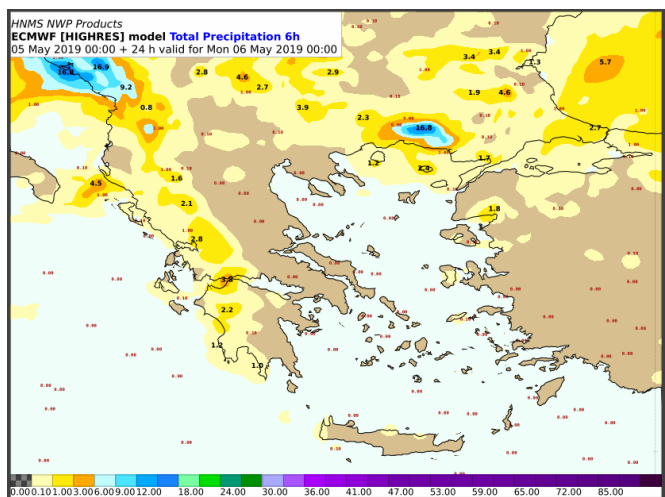
**6 HR TOTAL PRECIPITATIONS FORECAST FROM HRES ECMWF FOR 05-05-2019 06UTC**



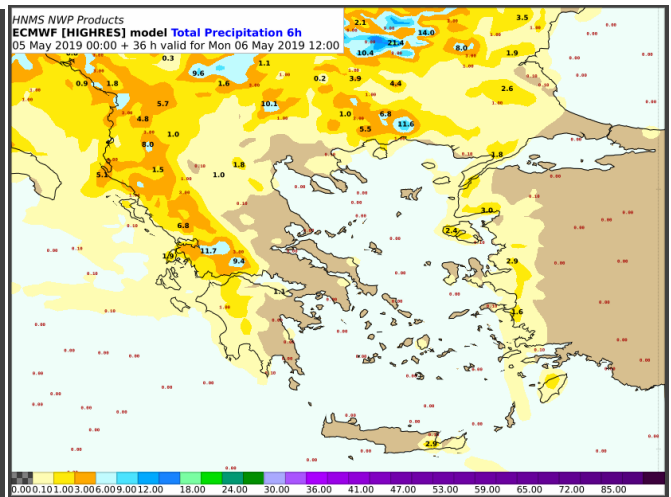
**6HR TOTAL PRECIPITATION FORECAST FROM HRES ECMWF FOR 05-05-2019 12UTC**



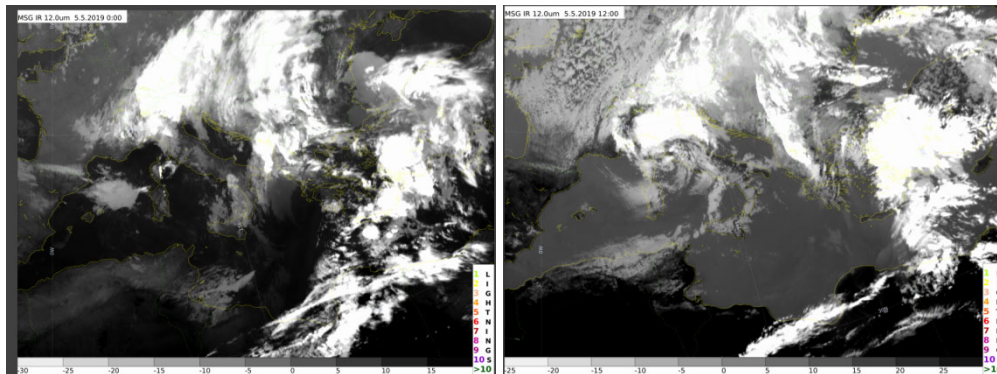
**6 HR TOTAL PRECIPITATIONS FORECAST FROM HRES ECMWF FOR 06-05-2019 00UTC**



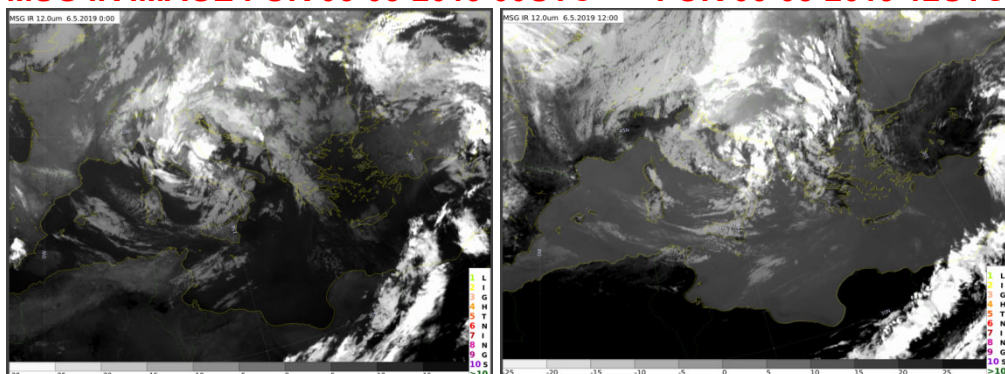
**6HR TOTAL PRECIPITATION FORECAST FROM HRES ECMWF FOR 06-05-2019 12UTC**



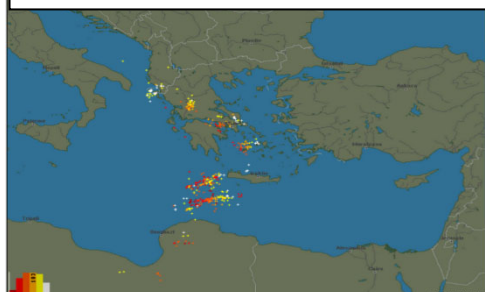
**MSG IR IMAGE FOR 05-05-2019 00UTC FOR 05-05-2019 12UTC**



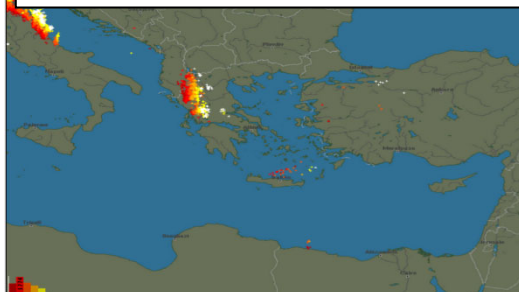
**MSG IR IMAGE FOR 06-05-2019 00UTC FOR 06-05-2019 12UTC**



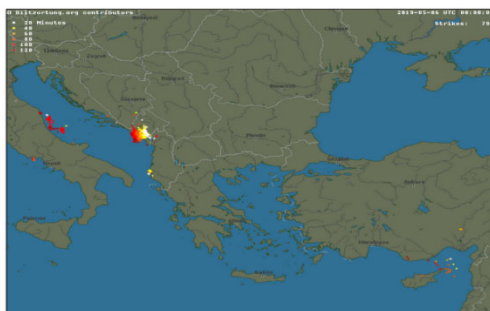
**LIGHTINGS ACTIVITY FOR 05-05-2019 00UTC**



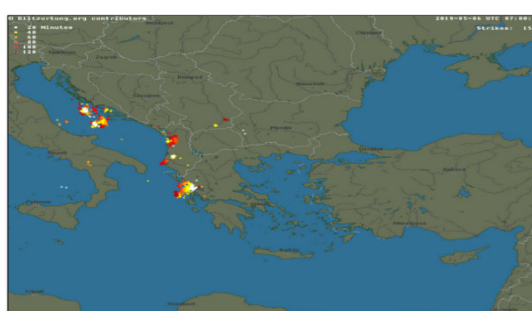
**LIGHTINGS ACTIVITY FOR 05-05-2019 12UTC**



**LIGHTINGS ACTIVITY FOR 06-05-2019 00UTC**



**LIGHTINGS ACTIVITY FOR 06-05-2019 07UTC**



**4. References to relevant publications**

Gofa, F., Boucouvala, D., Louka, P. and H Flocas , 2018: Spatial verification approaches as a tool to evaluate the performance of high resolution precipitation forecasts. *Atmospheric Research*, 208,, 78-87



## GREECE

**Prezerakos, N., Flocas, H. and S Michaelides S.** 1999: Upper tropospheric downstream development leading to surface cyclogenesis in the central Mediterranean. *Meteorol Appl* **6**:1–10.

**Lolis, C., Bartzokas, A and B. Katsoulis B.**, 2004: Relation between sensible and latent heat fluxes in the Mediterranean and precipitation in the Greek area during winter. *Int J Clim* **24**: 1803-1816.

**Kouroutzoglou, J., Avgoustoglou, E., Flocas, H., Hatzaki, M. Skrimizeas, P. and K. Keay**, 2018: Assessment of the role of sea surface fluxes on eastern Mediterranean explosive cyclogenesis with the aid of the limited-area model COSMO.GR, *Atmospheric Research* **208**:132-147